Title: HIV persists in late coronary atheroma and is associated with increased local inflammation and disease progression

Laventa M. Obare[1], Samuel S. Bailin[1], Xiuqi Zhang[1], Kisyua Nthenge[1], Stephen Priest[1], Qi Liu[2], Lindsey K Stolze[2], Quanhu Sheng[2], Rama Gangula[1], Madelaine Behrens[3], Brenita Jenkins[4], Praveena Prasad[4], Kit Neikirk[5], Prem Prakash[6,7,8], Meghan Hogan[9], Liang Zhang[10], Heather K. Beasley[5], Jianqiang Shao[10], Tyne W. Miller-Fleming[11], Kyera V. Actkins[11], Mark A. Phillips[12], David Hubert[12], Jordan Malone[1], Cassia Labeeb[1], Alexander Gelbard[13], Antoine Chaillon[14], Mona Mashayekhi[15], Curtis L. Gabriel[16], Tecla Temu[17], Lana Olson[18], Angela Jones[18], Karen Beeri[18], Paxton Baker[18], Kenji Kawai[19], Saikat Kumar B. Ghosh[19], Laing Guo[19], Renu Virmani[19], Aloke Finn[19], Palak Shah[19], Tzushan Sharon Yang[20], Alexander G. Bick[21], Annet Kirabo[6,22], Yan R Su[23], Elizabeth J. Phillips[1,24], Simon Mallal[1,24,25,26], Chandravanu Dash[7,8,9], John R. Koethe[1], Sara Gianella[2], Melanie R. McReynolds[5], Tarek Absi[27], Antentor Hinton[6], Celestine N. Wanjalla[1†]

[†]Corresponding author: Celestine N. Wanjalla, MD, Ph.D.; Division of Infectious Diseases, Vanderbilt University Medical Center, A-2200 MCN, 1161 21st Ave S., Nashville, TN, 37232-2582. (615) 322-2035 (o), (615) 343-6160 (f), celestine.wanjalla@vumc.org

Running Title: Spatial resolution of mechanisms in HIV-related atherosclerosis

Table S1. Demographics of coronary artery donors

	PLWH n=13	***PWoH n=15***
Age, yrs.	52.5 [46.5, 56.5]	51 [46.5, 60]
Sex, % Male	46.15	53.33
Race, % Caucasian	30.77	60
Plaque characteristics		
Early atheroma	4 (31%)	8 (53%)
PIT	2 (15%)	3 (20%)
Late atheroma	7 (54%)	4 (27%)
Vessel type, number	PLAD (4) PLAD1(2) PRC (1) PRC1 (1) MLAD (1) RCA2 (1) LOM (1) DLAD (1) MLAD1 (1)	PLAD (4) PRC1 (2) MRC3 (1) PLCX (1) DRC1 (1) PLAD5 (1) LD1 (1) LOM (1) MLAD (1) MRC (1) PRC2 (1)
Sudden death category	Cardiac death (6) Non-cardiac death: (4) Severe CAD w/o acute thrombus (2) Stent/CABG (1)	Cardiac death (5) Non-cardiac death (3) Severe CAD w/o acute thrombus (4) Unknown (1) Rupture (1) Erosion (1)

Abbreviations*: CAD – coronary artery disease; LOM1, Left obtuse marginal artery 1; MLAD, middle left anterior descending coronary artery; MRC, middle segment of RCA; PIT, Pathologic intimal thickening; PLAD1, proximal left anterior descending obstruction; PLC, proximal left circumflex; PRC-1, proximal right coronary artery 1*

Chronic total occlusion (HIV-negative) plaque excluded from statistical analysis comparing HIV-positive and HIV-negative IHC plaques

Table S2. Demographics of Aorta Donors

	PLWH ***n=5***	***Without HIV*** ***n=17***
Age, yrs.	64.0 [44.0 – 68.5]	66.0 [60, 70.5]
Sex, % Male	4 (80%)	11 (64.7%)
Race, % Caucasian	4 (80%)	15 (88.2%)
BMI, Kg/m^2	23.8 [20.3, 30.6]	30.9 [24.6, 40.2]
With Diabetes	1 (20%)	1 (0.06%)
Smoking history	1 (20%)	9 (52.9%)
Aorta Characteristics		
Location of Aorta	Thoracic aorta (4) Not specified (1)	Thoracic aorta (10) Not specified (6) Abdominal (1)
Time to processing, hrs.	14.7 [11.9, 21]	13.3 [10.2, 16.4]
Cause of death	Respiratory arrest, Pulmonary edema Cancer HIV Respiratory failure (PEs) Cardiac arrest	Self-inflicted GSW Natural cardiac death CVA/Stroke (6) Intracranial hemorrhage Cardiopulmonary arrest (5) Respiratory failure Trauma End-stage COPD

Abbreviations*: BMI, body mass index; yrs., years; hrs., hours; GSW, gunshot wound; CVA, cerebral vascular accident*

Table S3. Immune cells by atheroma type.

	N	Early atheroma *N=12*	Late atheroma *N=11*	PIT *N=5*	Combined *N=28*	Test Statistic
% CD68	17	0.7 [0.4, 1.41]	1.5 [0.4, 3.3]	0.2 [0.2, 0.30]	0.7 [0.2, 1.9]	0.2
% CD163	28	0.2 [0.02, 0.3]	**0.5 [0.2, 1.04]**	0.03 [0.009, 0.2]	0.2 [0.03, 0.6]	**0.04**
% CD3	28	**0.5 [0.3, 0.6]**	0.3 [0.3, 0.5]	0.1 [0.07, 0.2]	0.3[0.2, 0.5]	**0.02**
% CD4	28	0.1[0.03, 0.2]	0.1[0.04, 0.3]	0.03[0.01, 0.04]	0.08[0.03, 0.2]	0.2
% CD8	18	0.2[0.06, 0.3]	0.1[0.06, 0.2]	0.07[0.04, 0.09]	0.1[0.04, 0.2]	0.3
% VCAM-1	28	0.08[0.02, 0.2]	0.2[0.06, 0.3]	0.09 [0.09, 0.2]	0.09[0.04, 0.2]	0.8
% CX3CR1	27	0.7 [0.3, 1.2]	0.7 [0.5, 0.9]	0.5[0.3, 0.7]	0.7 [0.4, 1.0]	0.5
Plaque area (um2)	28	5908380[446006,47668736]	**7854450[6803160, 9405144]**	3451790[2632771, 3797240]	6276039 [4361691, 7966864]	**0.001**
% Stenosis	28	68 [61, 79]	**79 [62, 82]**	50 [42, 52]	67[53, 80]	**0.006**
% STING	23	0.3[0.2, 0.7]	0.1 [0.04, 0.5]	0.3 [0.2, 0.5]	0.2[0.08, 0.6]	0.3
% GZMB	23	**0.2 [0.1, 0.3]**	0.09 [0.04, 0.09]	0.12 [0.07, 0.2]	0.1 [0.06, 0.20]	**0.04**

***B [a,c]* represent the lower quartile *a*, the median *b*, and the upper quartile *c* for continuous variables.**
Test used: Kruskal-Wallis test .

Table S4. CHIP calls

	CHIP	TOP GENE	TOP GENE VARIANT	ATHEROMA	CULPRIT VESSEL	AGE	RACE	SEX
PLWH	YES	TP53	C275Y	Pathologic Intimal Thickening	MLAD1	48	Black	Male
	NO			Late Fibroatheroma	DLAD	64	Black	Male
	YES	ASXL1	Q1039X	Late Fibroatheroma	PLAD1	55	White	Female
	YES	DNMT3A	W440X	Early Fibroatheroma	PLAD1	54	Black	Female
	NO			Late Fibroatheroma	PRC1	40	Black	Male
	YES	TP53	C277Y	Late Fibroatheroma	RCA2	44	Asian	Male
	NO			Early Fibroatheroma	PRC	49	Black	Male
	NO			Late Fibroatheroma	LOM	57	Black	Female
	YES	TET2	G1275E	Early Fibroatheroma	MLAD	44	Black	Female
	NO			Pathologic Intimal Thickening	PLAD	52	Black	Female
	YES	TET2	P1866S	Early Fibroatheroma	PLAD	57	Black	Male
	NO			Late Fibroatheroma	PLAD	54	White	Female
PWoH	NO				RCA, MLAD	42	White	Male
	YES	ASXL1	Q623X	Early Fibroatheroma	PLAD	43	White	Male
	NO			Early Fibroatheroma	PLAD	58	Black	Male
	NO			Early Fibroatheroma	PLCX	55	Black	Male
	YES	TET2	R550X	Late Fibroatheroma	PLAD	44	Asian	Male
	NO			Pathologic Intimal Thickening	MLAD	51	Black	Male
	YES	TET2	C1374Y	Late Fibroatheroma	LOM	55	White	Female
	NO			Pathologic Intimal Thickening	MRC	62	Black	Female
	YES	ASXL1	Q1286X	Early Fibroatheroma	DRC1	46	Black	Male
	NO			Late Fibroatheroma	LD1	54	White	Female

Figure S1. Characterization of coronary plaques.

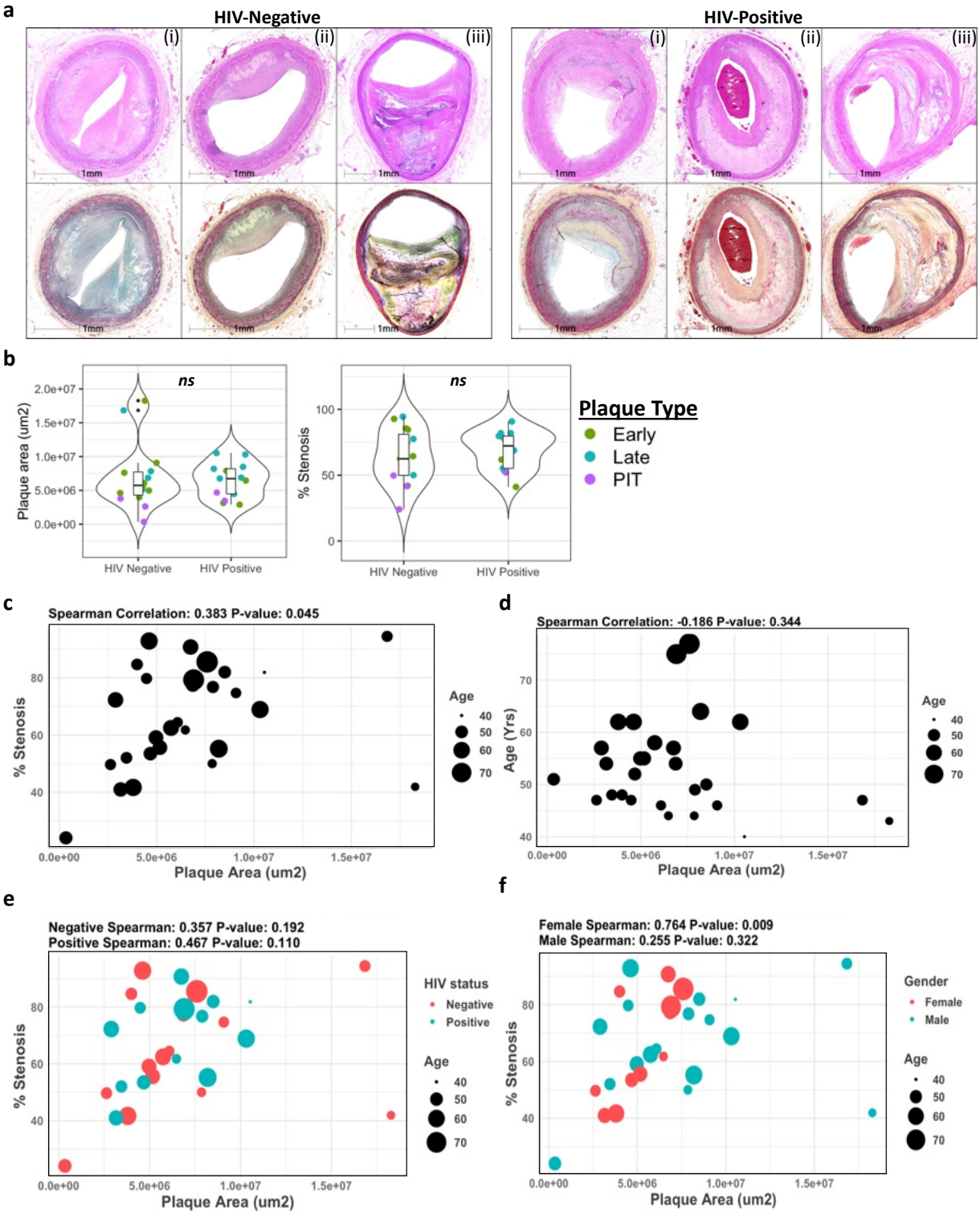

a, Representative coronary plaques from three PLWH and three PWoH were stained with H&E and Movat stain. **b**, Plaque area (μm^2) and % plaque stenosis were measured and calculated in coronary arteries from 13 deceased PLWH and 15 PWoH. Violin plots with jitter show plaque area and plaque stenosis distribution by HIV status. **c**, Correlation plot between arterial stenosis and plaque area, depicting patient age. **d**, Correlation plot between arterial stenosis and age. **e**, Correlation plot stratified by HIV status and **f**, sex. Statistical analysis, Wilcoxon test, and Spearman correlation.

Figure S2. Coronary plaque immune cell constituents in HIV-positive and HIV-negative persons.

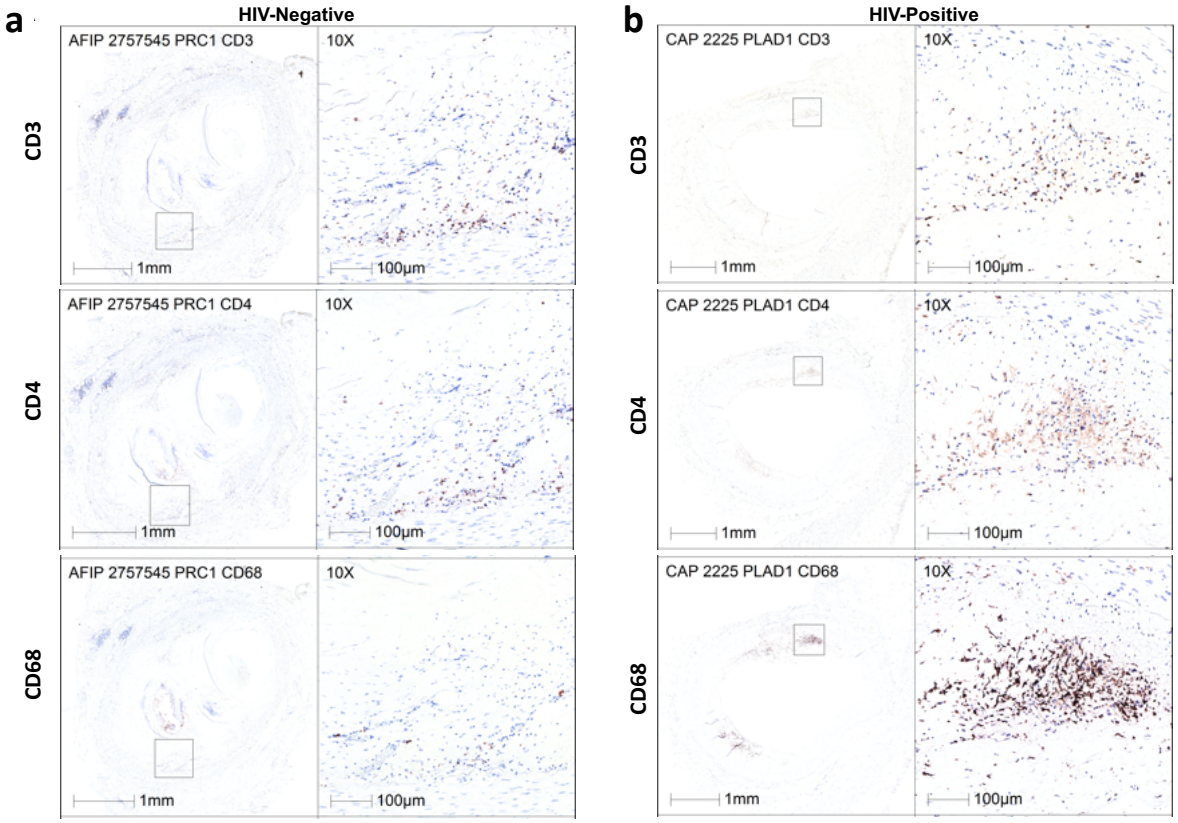

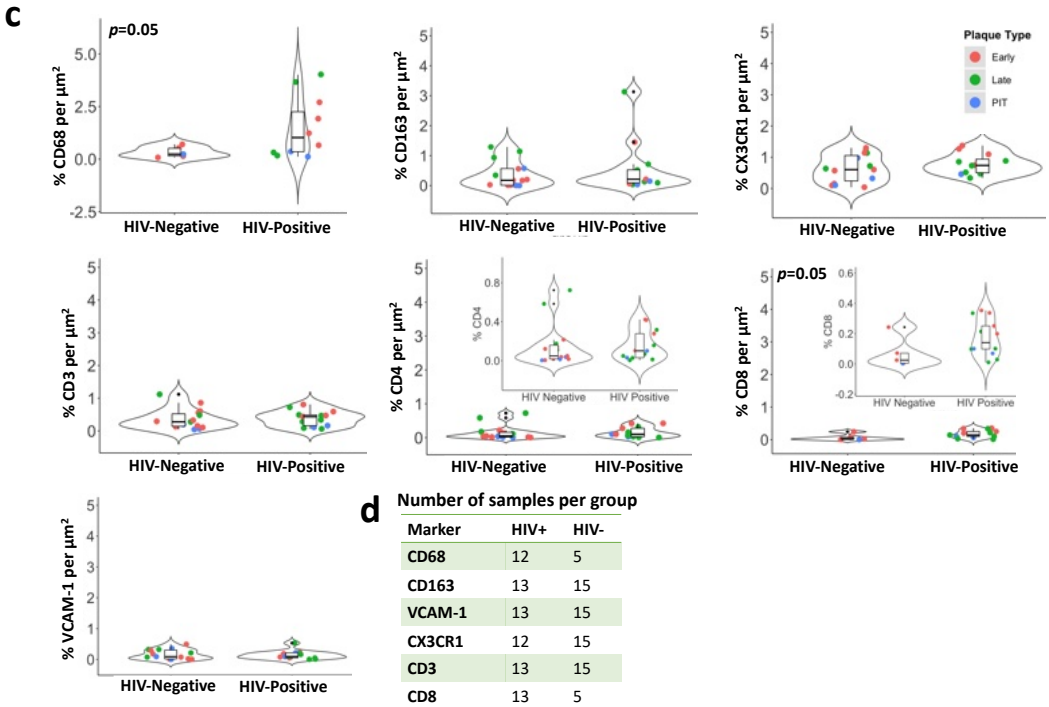

d Number of samples per group

Marker	HIV+	HIV-
CD68	12	5
CD163	13	15
VCAM-1	13	15
CX3CR1	12	15
CD3	13	15
CD8	13	5
CD4	13	15

a, IHC stains of CD3, CD4, and CD68, in early fibroatheroma of one representative coronary plaque from HIV-negative and **b**, HIV-positive deceased donors. **c**, IHC stains were quantified as % of stain per um^2 of coronary plaque; CD68, CD163, VCAM-1, CX3CR1, CD3, CD4, and CD8 were measured. **d**, Plaque type is indicated by color, early fibroatheroma (red), late fibroatheroma (green), and pathologic intimal thickening (blue). The number of samples quantified per group is shown. Statistical analysis, Wilcoxon test

Figure S3. HIV copies are associated with coronary artery inflammation.

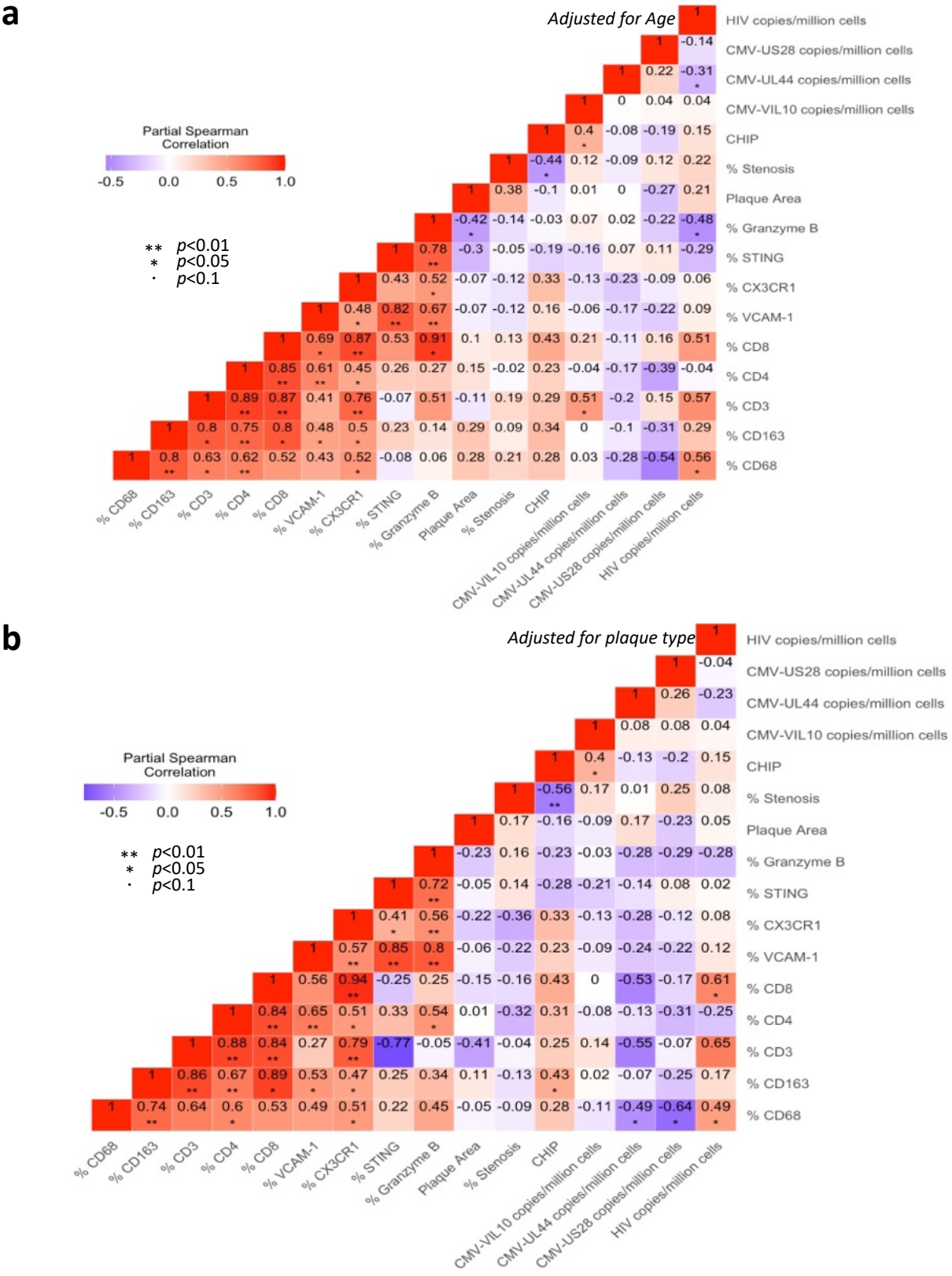

a, Partial Spearman correlation plots of % immune markers expressed/um^2 in coronary plaques from all donors (n=28) adjusted for age and **b**, plaque type. * p< 0.05, p<=0.01, *** p<=0.001, **

Figure S4. CMV transcripts are not significantly higher in medium-sized coronary arteries of PLWH than PWoH.

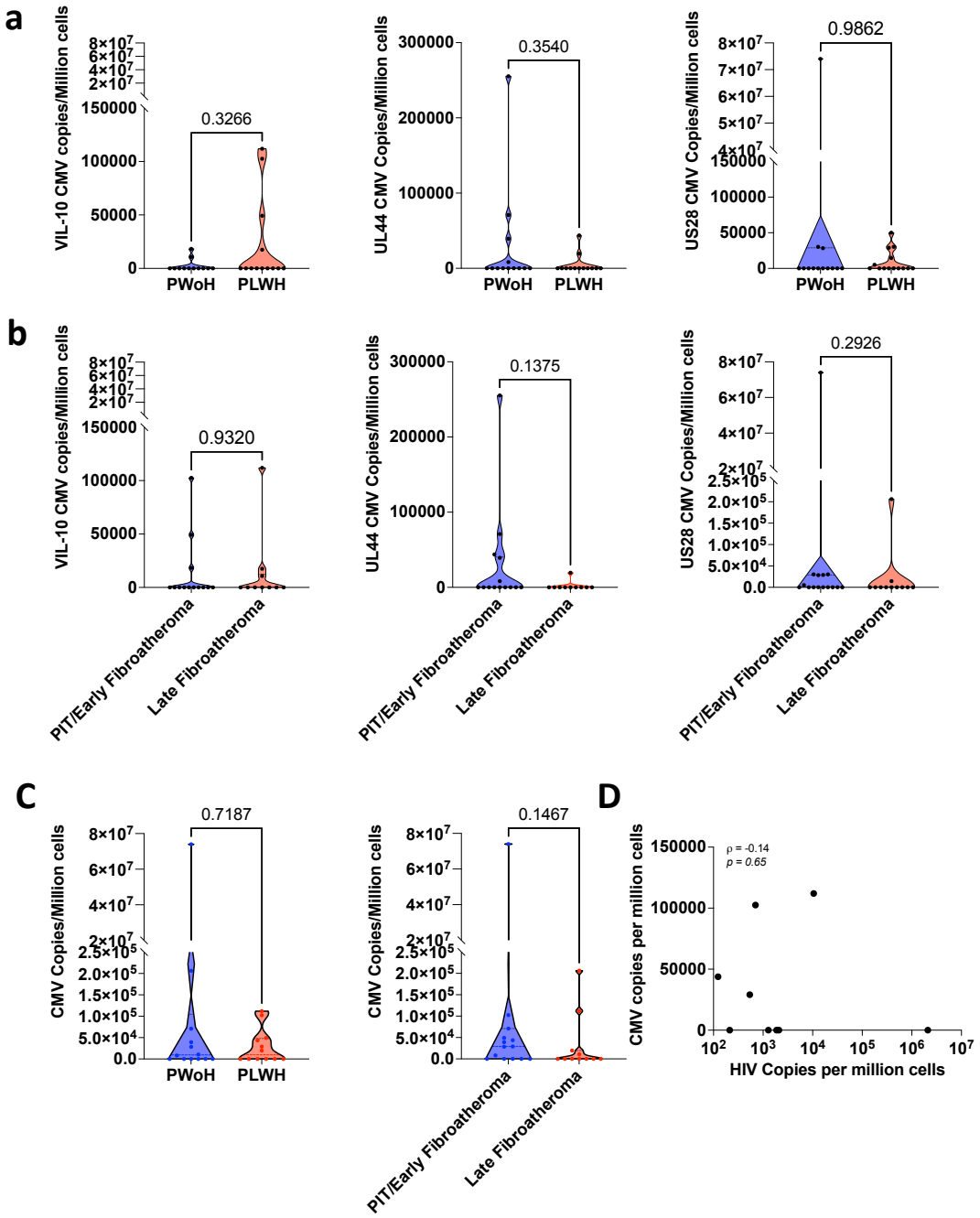

a, We quantified CMV copies using droplet digital PCR using primers against VIL-10, UL44, and US28. **b**, Comparisons by atheroma stage. **c**, Total CMV copies by HIV status and atheroma stage. **d**, Correlation plot shows the relationship between HIV and CMV copy number. Statistical analysis by Mann Whitney U test and Spearman correlation analysis.

* p< 0.05, p<=0.01, *** p<=0.001, **** p<=0.0001

Figure S5. Immunofluorescence images of twelve ROIs per sample (HIV-negative and positive) showed every marker (CD68, CD3, CD8) and DAPI stain used to select ROIs.

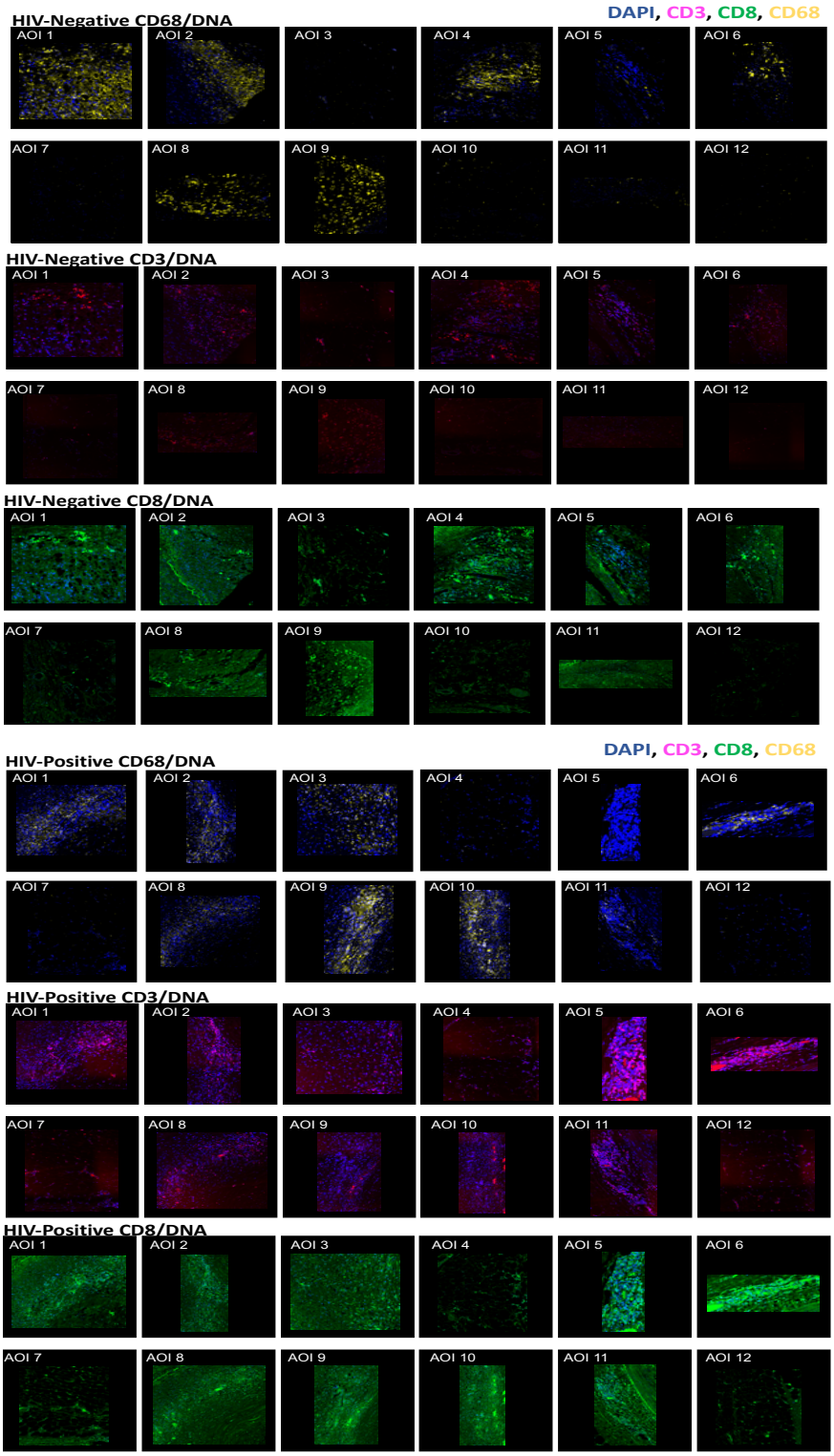

Figure S6. Signal-to-noise ratio normalized barcode counts of the three fluorescently tagged markers across all 12-AOIs.

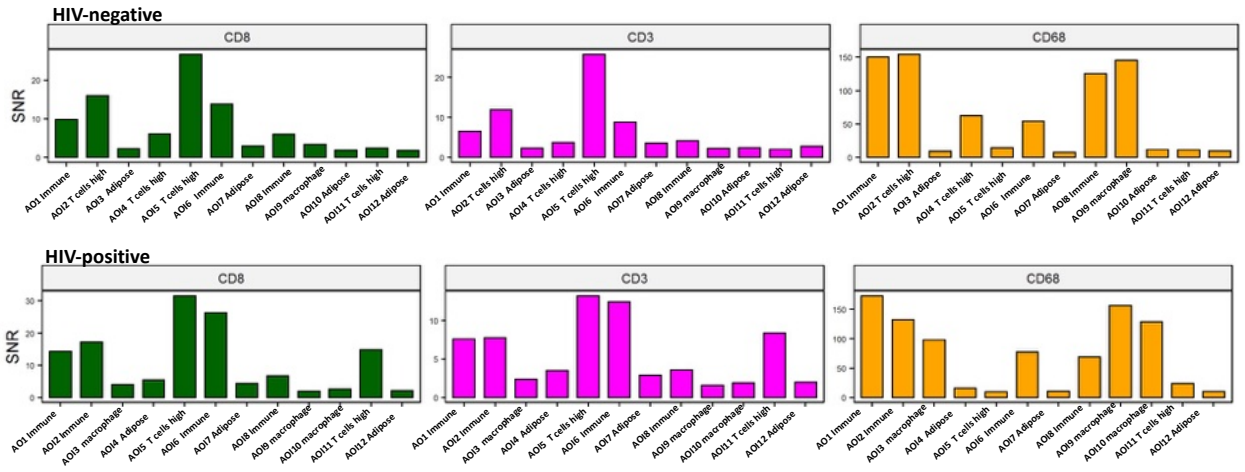

Figure S7. Spatial graphing depicts the relative gene expression of CD163 in AOIs.

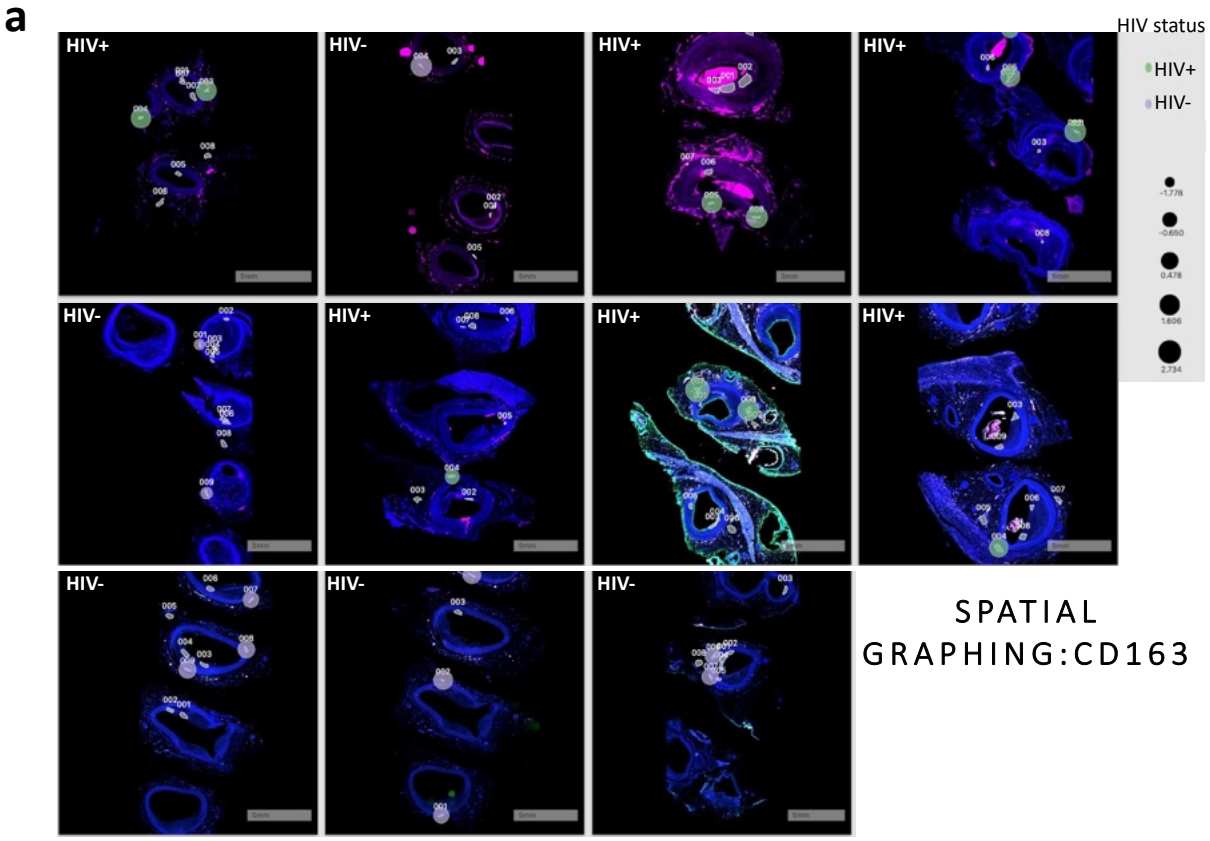

Magenta stain shows expression of $CD45^{+}$ immune cells in the AOIS. Low magnification images from coronaries of PLWH (green circles) and PWoH (blue circles) (A) and high magnification (B). Two representative AOIs are shown at high resolution, with the green and blue circle inset depicting higher expression of CD163 in the AOI from PLWH compared to coronary from PWoH in the adventitia area near the adipocytes.

Figure S8. CD163 and CD209 expression are positively correlated in the aorta from PLWH.

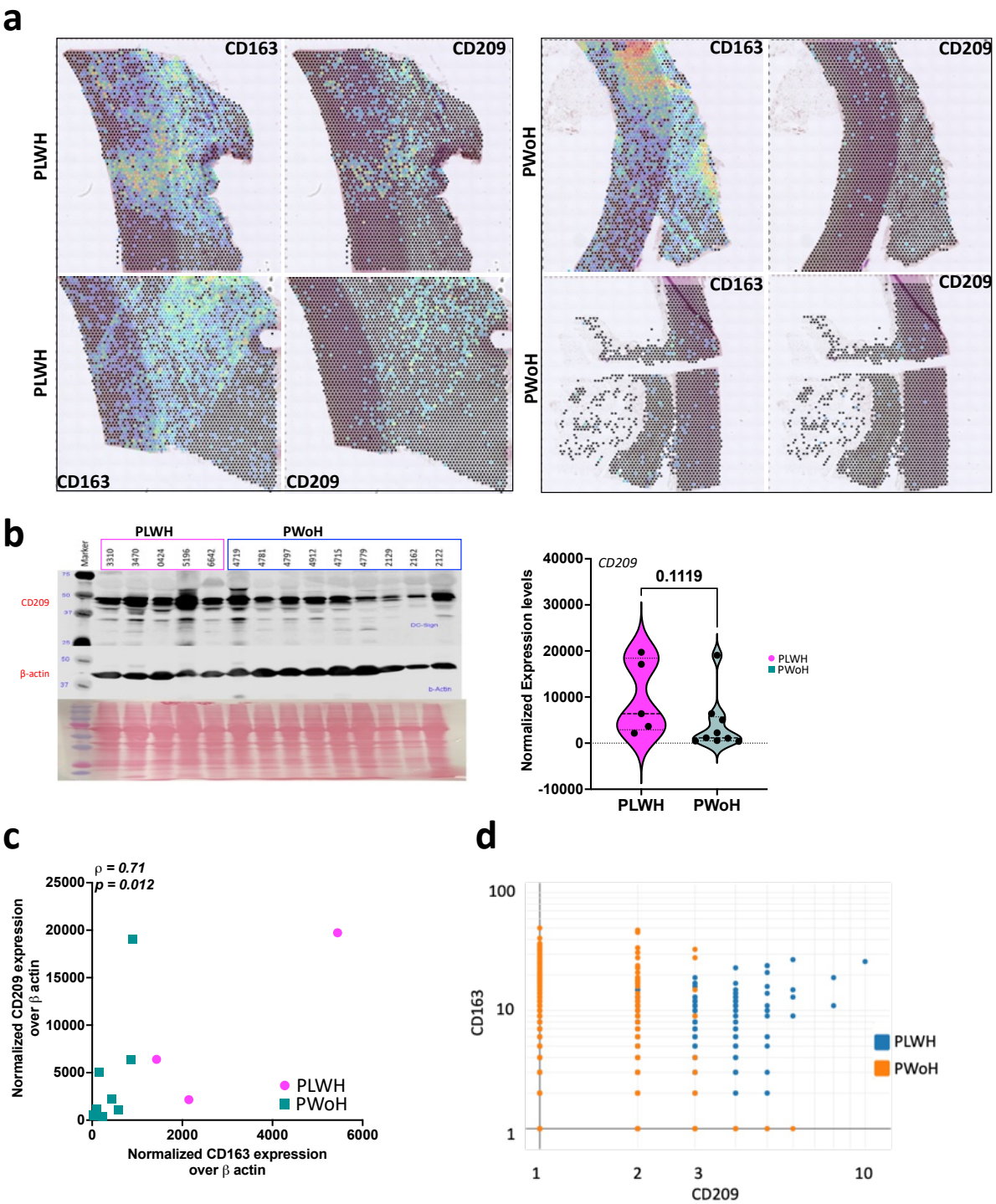

a, CD163 and CD209 gene transcripts are shown in PLWH and PWoH. **b**, Western blot shows expression of CD209, quantified on the right after normalization based on actin. **c**, CD163/CD209 protein, and **d**, gene transcript expression correlated. Mann-Whitney U test and Spearman rank correlated used in b and c.

Figure S9. Classification of immune cell clusters from CosMX analysis

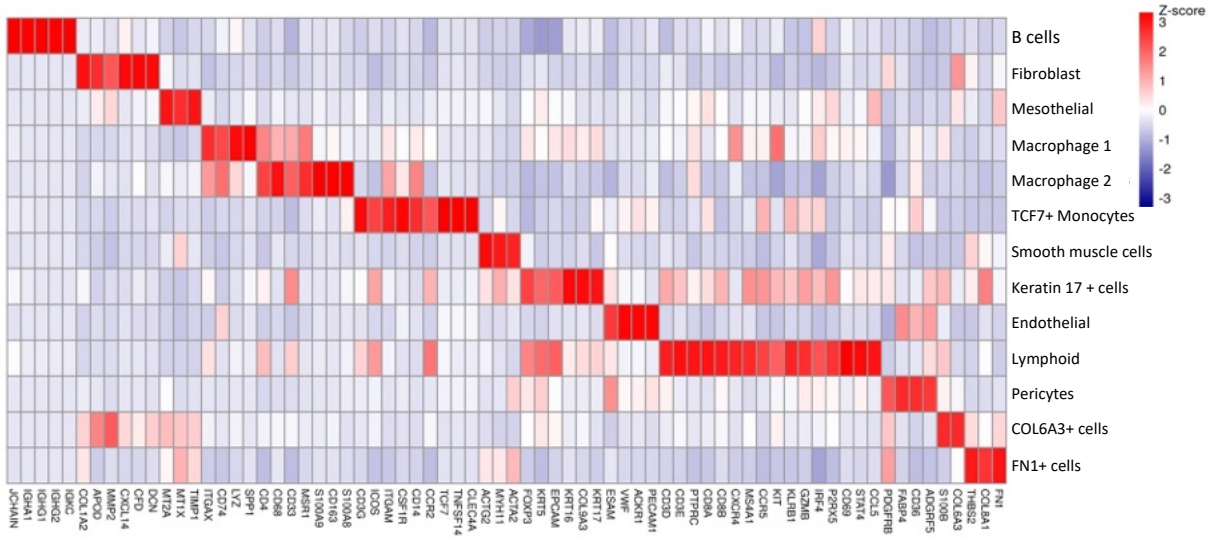

Heatmap shows differentially expressed genes in all clusters of cells delineated by machine learning algorithms from CoSMX analysis of coronary arteries from PLWH and PWoH.

Figure S10. Niche 7 is in the atheroma and contains the highest expression of CXCR4

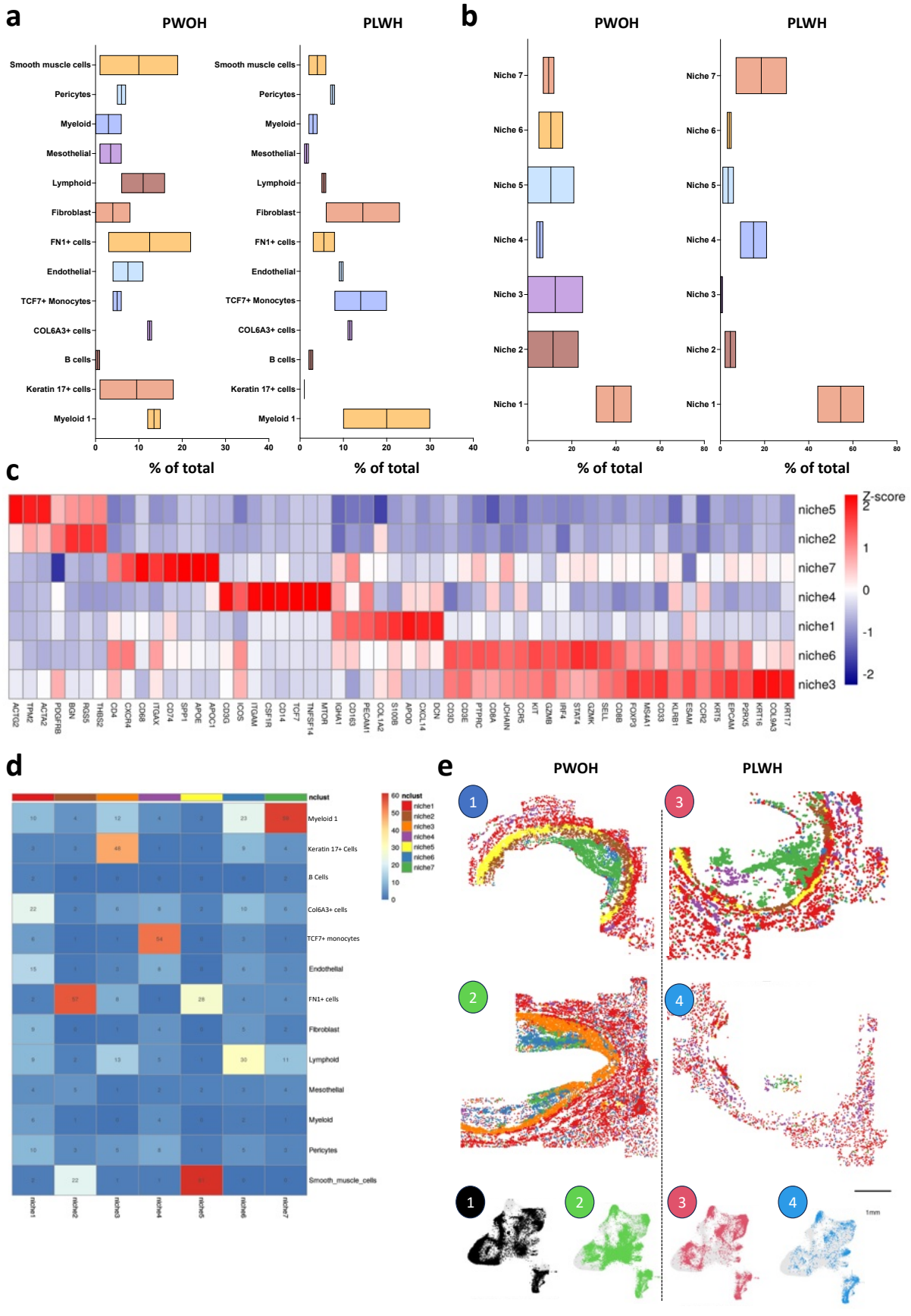

a, Box plots show the proportions of the different cell clusters. **b**, and spatial niches in coronary arteries with late atheroma from PWoH (n=two) and PLWH (n=two). c, Heatmap shows differentially expressed genes in all niches. d, The different cell clusters present within each niche are shown in the heatmap. e, Spatial niches are shown within the coronary arteries. Each coronary artery is numbered to correspond with concatenated UMAP, showing the contribution of each coronary section (based on fov's selected) to the UMAPs.

Figure S11. SPP1 among highly expressed molecules in niche 7 of coronary arteries from PLWH and PWoH

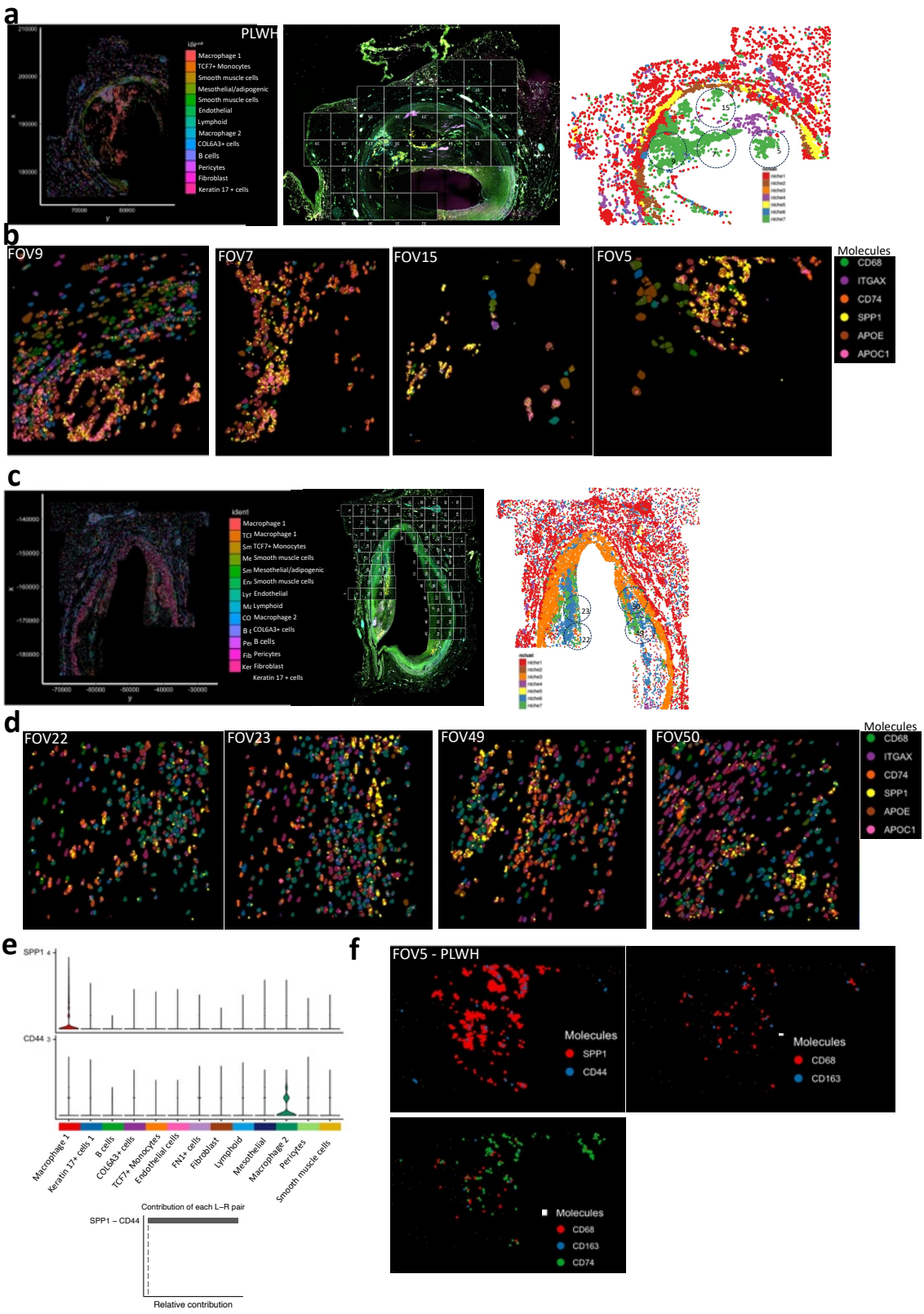

a, Coronary artery from PLWH showing cells resolved with single-cell resolution (left), fov's selected on FFPE samples (middle), and niches identified within the selected focus (right). **b**, Molecules previously shown to be highly expressed in niche seven, CD68, ITGAX, CD74, SPP1, APOE, and APOC1 are depicted within selected fovs of niche seven. **c,** Coronary artery from PWoH showing cells resolved with single-cell resolution (left), fov's selected on FFPE samples (middle), and niches identified within the selected focus (right). **d**, Molecules previously shown to be highly expressed in niche seven. **e**, CellChat predicts ligand-receptor interactions between SPP1 and CD44 on macrophages (left and middle). f, Fov five from (a) was selected to show CD44 (blue) and SPP1 (red) molecules (left) and CD68/CD163 (right) depicting macrophages within the same fov and with the addition of CD74 molecules (bottom).